

Thermodynamical quantities of lattice full QCD from an efficient method

Xiang-Qian Luo

Department of Physics, Zhongshan University, Guangzhou 510275, China

November 14, 2018

Abstract

I extend to QCD an efficient method for lattice gauge theory with dynamical fermions. Once the eigenvalues of the Dirac operator and the density of states of pure gluonic configurations at a set of plaquette energies (proportional to the gauge action) are computed, thermodynamical quantities deriving from the partition function can be obtained for arbitrary flavor number, quark masses and wide range of coupling constants, without additional computational cost. Results for the chiral condensate and gauge action are presented on the 10^4 lattice at flavor number $N_f = 0, 1, 2, 3, 4$ and many quark masses and coupling constants. New results in the chiral limit for the gauge action and its correlation with the chiral condensate, which are useful for analyzing the QCD chiral phase structure, are also provided.

1 Introduction

Although it is believed to be the most powerful non-perturbative approach to quantum field theory, lattice Monte Carlo techniques still suffer from systematic errors. The sources of systematic error are mainly finite size effects, finite lattice spacing, quenched approximation, and the use of unphysical quark masses. Finite volume effects and lattice spacing errors are relevant, and can be significantly reduced through the implementation of the Symanzik improvement [1, 2, 3, 4, 5, 6, 7, 8]. Quenched approximation ignores the feedback of fermions (the determinant of the Dirac operator Δ in the measure is constraint to be $\det \Delta = 1$). More recent investigations [9, 10, 11] suggest that quenched approximation may lead to a systematic deviation from experiment.

The most popular algorithms for generating unquenched configurations are the hybrid Monte Carlo (HMC) [12] and/or hybrid molecular dynamics (HMD) algorithms [13]. In these algorithms, each trial configuration is generated by solving the equation of motion with some number of steps, and in each step, numerical inversion of the Dirac matrix

has to be done. For a different set of bare parameters of “sea” quark mass m_{sea} , flavor number N_f , and coupling constant g , new independent simulations are required. Therefore, these algorithms are still very expensive and require high performance supercomputers, in particular for small quark masses, even on a moderate lattice.

Without loss of generality, let us discuss the unimproved lattice QCD with Kogut-Susskind quarks, which has the action $S = S_g + S_f$. Here

$$\begin{aligned}
S_g &= -\frac{\beta}{N_c} \sum_p \text{ReTr}(U_p), \\
S_f &= \sum_{x,y} \bar{\psi}(x) \Delta_{x,y} \psi(y), \\
U_p &= U_\mu(x) U_\nu(x + \mu) U_\mu^\dagger(x + \nu) U_\nu^\dagger(x), \\
\Delta_{x,y} &= m \delta_{x,y} \\
&\quad + \frac{1}{2} \eta_\mu(x) \left[U_\mu(x) \delta_{x,y-\mu} - U_\mu^\dagger(x - \mu) \delta_{x,y+\mu} \right], \\
\eta_\mu(x) &= (-1)^{x_1+x_2+\dots+x_{\mu-1}}.
\end{aligned} \tag{1}$$

The bare coupling constant g is related to β by $\beta = 2N_c/g^2$ with $N_c = 3$ the number of colors. The corresponding partition function is

$$\mathcal{Z} = \int [dU] e^{-S_g} (\det \Delta(m, U))^{N_f/4}. \tag{2}$$

In most simulations, people (e.g. [14]) usually distinguish “sea” quarks (for the configurations) from the “valence” quarks (for the quark propagators), due to the heavy costs in generating the full QCD configurations at different set of sea quark masses. Let us take the chiral condensate as an example, which is meant to compute

$$\langle \bar{\psi} \psi \rangle = \frac{\int [dU] \text{Tr} \Delta^{-1}(m_{val}, U) e^{-S_g} (\det \Delta(m_{sea}, U))^{N_f/4}}{V N_c \int [dU] e^{-S_g} (\det \Delta(m_{sea}, U))^{N_f/4}} \tag{3}$$

at a set of valence quark mass m_{val} , while always using a full configuration at a given sea quark mass $m_{sea} \neq m_{val}$. Unfortunately, this distinction is not theoretically consistent with the physical case $m = m_{val} = m_{sea}$.

In this work, I will describe an efficient method for simulating lattice QCD with dynamical fermions, which is particularly useful for investigating the thermodynamical properties and chiral properties. Results will be provided for the chiral condensate and gauge action in QCD on the 10^4 lattice for flavor number $N_f = 1, 2, 3, 4$, and many values of quark mass m and coupling constant g . New results in the chiral limit for the gauge action and its correlation with the chiral condensate will also be presented.

2 METHODOLOGY

The method described here is a generalization of the microcanonical fermionic average method [15] to QCD in 3+1 dimensions. Using the identity

$$e^{-S_g} = \int dE \delta \left(\frac{1}{N_c} \sum_p \text{ReTr}(U_p) - 6VE \right) e^{6V\beta E}, \quad (4)$$

one can rewrite the partition function as a one-dimensional integral

$$\mathcal{Z} = \int dE e^{-S^{\text{eff}}(E, m, N_f, \beta)}. \quad (5)$$

Here S^{eff} is the full effective action as a function of plaquette energy E , quark mass m , flavor number N_f , and coupling β defined by

$$\begin{aligned} S^{\text{eff}}(E, m, N_f, \beta) &= -\ln n(E) - 6\beta VE \\ &+ S_f^{\text{eff}}(E, m, N_f), \end{aligned} \quad (6)$$

where V is the total number of lattice sites,

$$n(E) = \int [dU] \delta \left(\frac{1}{N_c} \sum_p \text{ReTr}(U_p) - 6VE \right) \quad (7)$$

is the density of states at the given E , and

$$\begin{aligned} S_f^{\text{eff}} &= -\ln \langle (\det \Delta(m, U))^{N_f/4} \rangle_E \\ &= -\ln \left\langle \left(\prod_{i=1}^{N_c V/2} (\lambda_i^2(U) + m^2) \right)^{N_f/4} \right\rangle_E \end{aligned} \quad (8)$$

is the effective fermionic action. Non-vanishing S_f^{eff} implies the interaction between quarks and gluons. Here $\lambda_i(U)$ is the i -th positive eigenvalue of the massless Dirac operator $\Delta(m=0)$ and $\langle \dots \rangle_E$ is the average of the observable over configurations with the probability distribution $\delta \left(\sum_p \text{ReTr}(U_p)/N_c - 6VE \right) / n(E)$ at fixed plaquette energy E . S_f^{eff} does not depend on β . Once I compute the the positive eigenvalues of $\Delta(m=0)$ for *pure gauge* configurations at a set of E , I can obtain at no cost S_f^{eff} and therefore the partition function for any m , N_f and β . Then the thermodynamical properties can be obtained from the derivatives of the partition function. For example the chiral condensate and the vacuum expectation value of the plaquette are

$$E_p = \frac{\langle \text{Re Tr} U_p \rangle}{N_c} = \frac{1}{6V} \frac{\partial \ln \mathcal{Z}}{\partial \beta}$$

$$\begin{aligned}
&= \frac{\int dE E e^{-S^{\text{eff}}(E,m,N_f,\beta)}}{\mathcal{Z}}, \\
\langle \bar{\psi}\psi \rangle &= \frac{1}{VN_c N_f/4} \frac{\partial \ln \mathcal{Z}}{\partial m} \\
&= \frac{-1}{VN_c N_f/4} \frac{\int dE \frac{\partial S_f^{\text{eff}}}{\partial m} e^{-S^{\text{eff}}(E,m,N_f,\beta)}}{\mathcal{Z}} \\
&= \frac{1}{VN_c \mathcal{Z}} \int dE e^{-S^{\text{eff}}(E,m,N_f,\beta)} \\
&\times \frac{\langle \sum_{i=1}^{N_c V/2} \frac{2m}{\lambda_i^2(U)+m^2} (\det \Delta(m,U))^{N_f/4} \rangle_E}{\langle (\det \Delta(m,U))^{N_f/4} \rangle_E}. \tag{9}
\end{aligned}$$

We can also calculate the specific heat, chiral susceptibility and other local quantities. One prominent feature is that the effective action and partition function are also calculable in the chiral limit, which is very useful for studying the chiral properties.

3 IMPLEMENTATION

The basic idea of the algorithm described in Sect. 2 is to compute the effective action in Eq. (6). The density of states $n(E)$ can be directly evaluated by numerically integrating out the quenched SU(3) data:

$$-\frac{\ln n(E)}{V} = 6 \int_0^E dE' \beta(E', N_f = 0) + \text{const.} \tag{10}$$

The most important and time consuming part of the work, is the computation of S_f^{eff} in Eq. (8) by averaging out the fermionic determinant over configurations at the given E . These configurations can be generated by microcanonical or over-relaxation processes. For SU(3), although there exists a microcanonical algorithm [16], it is very difficult to implement it ergodically. To solve the problem, I use a different prescription, over-relation-updating the subgroups SU(2) of SU(3) described as follows. Let U be an SU(3) link to be updated, and R the sum of 6 staples.

(a) Find the 2×2 block of UR by striking out the 3rd row and column [17]:

$$\begin{pmatrix} B_1 & B_3 & \times \\ B_2 & B_4 & \times \\ \times & \times & \times \end{pmatrix}. \tag{11}$$

Write

$$B = r_0 + i\vec{r} \cdot \vec{\sigma} = \begin{pmatrix} B_1 & B_3 \\ B_2 & B_4 \end{pmatrix}, \tag{12}$$

with r_0 and \vec{r} being complex. Then find B' , and the norm k :

$$\begin{aligned} B' &= \text{Re}(r_0) + i\text{Re}(\vec{r}) \cdot \vec{\sigma} \\ &= \begin{pmatrix} (B_1 + B_4^*)/2 & (B_3 - B_2^*)/2 \\ (B_2 - B_3^*)/2 & (B_1^* + B_4)/2 \end{pmatrix}, \\ k &= \sqrt{\det B'}, \end{aligned} \tag{13}$$

so that B'/k is a $\text{SU}(2)$ matrix. Denote

$$C = ((B')^\dagger/k)^2 = \begin{pmatrix} C_1 & C_3 \\ C_2 & C_4 \end{pmatrix}, \tag{14}$$

and

$$a_1 = \begin{pmatrix} C_1 & C_3 & 0 \\ C_2 & C_4 & 0 \\ 0 & 0 & 1 \end{pmatrix}. \tag{15}$$

Perform over-relaxation updates [18] of the $\text{SU}(2)$ subgroups: $U' = a_1 U$.

(b) Find the 2×2 block of $U'R$ by striking out the 2nd row and column:

$$\begin{pmatrix} B_1 & \times & B_3 \\ \times & \times & \times \\ B_2 & \times & B_4 \end{pmatrix}, \tag{16}$$

Repeat the procedure of finding C as Eqs. (12), (13), (14) and denote

$$a_2 = \begin{pmatrix} C_1 & 0 & C_3 \\ 0 & 1 & 0 \\ C_2 & 0 & C_4 \end{pmatrix}, \tag{17}$$

$U'' = a_2 U'$.

(c) Find the 2×2 block of $U''R$ by striking out the 1st row and column:

$$\begin{pmatrix} \times & \times & \times \\ \times & B_1 & B_3 \\ \times & B_2 & B_4 \end{pmatrix}. \tag{18}$$

Repeat the procedure of finding C as Eqs. (12), (13), (14) and denote

$$a_3 = \begin{pmatrix} 1 & 0 & 0 \\ 0 & C_1 & C_3 \\ 0 & C_2 & C_4 \end{pmatrix}. \tag{19}$$

The new link is now $U_{new} = a_3 U''$. The processes above satisfy $\text{Tr}(U_{new}R) = \text{Tr}(U''R) = \text{Tr}(U'R) = \text{Tr}(UR)$, where the plaquette energy remains unchanged.

The Lanczos algorithm [19] was designed for calculating the eigenvalues of a large sparse matrix, but the rounding errors grow exponentially for the larger eigenvalues. I use the modified Lanczos algorithm [20, 21] to solve this problem so that all the true eigenvalues can be found. On a d dimensional lattice with V lattice sites, the following sum rules

$$\begin{aligned} \sum_{i=1}^{N_c V/2} \lambda_i^2 &= N_c V, \\ \sum_{i=1}^{N_c V/2} \lambda_i^4 &= \left[\frac{4d-1}{2} - (d-1)E \right] \frac{dN_c^2 V}{8} \end{aligned} \quad (20)$$

can be used to check the accuracy of the eigenvalues of $\Delta(m=0)$.

4 RESULTS

4.1 Microcanonical updates

I describe now the QCD data on the 10^4 lattice, obtained on a workstation. For the gauge fields, periodic boundary conditions are used. For fermions anti-periodic boundary condition in the time direction is implemented.

First, I calculate the quenched mean plaquette energy as a function of β , using the Cabibbo-Marinari [17] algorithm. High precision for this quantity can be easily achieved. Figure 1 shows the result. Then I calculate the density of states using Eq. (10), by numerically integrating out the interpolated data for $\beta(E)$ according to the trapezoidal rule. The result is shown in Fig. 2, while the irrelevant constant in Eq. (10) is ignored.

At each fixed E , 10000-40000 pure gauge configurations are generated, each one is separated by 100 over-relation updates. 100-400 de-correlated configurations are used for the diagonalization of the massless Kogut-Susskind fermionic matrix $\Delta(m=0)$. Their eigenvalues are stored on a disk with double precision, and the relative errors of the sum rules in Eq. (20) are the order of 10^{-8} and 10^{-7} respectively. Figure 3 plots the quenched chiral condensate

$$\langle \bar{\psi}\psi \rangle = \frac{\int dE n(E) e^{6\beta V E} \langle \sum_{i=1}^{N_c V/2} \frac{2m}{\lambda_i^2(U)+m^2} \rangle_E}{V N_c \int dE n(E) e^{6\beta V E}} \quad (21)$$

versus m at $\beta = 6.05$. The results are in good agreement with Chen's data [22], although Chen used the fermionic matrix inversion method on a much larger lattice $16^3 \times 32$. This provides an additional check of the eigenvalues.

From the eigenvalues of $\Delta(m=0)$ at 16 values of $E \in [0, 1)$, we can compute the effective fermionic action in Eq. (8) at any m and N_f at almost no cost. Figures 4,5,6, and

7 show the effective fermionic action (normalized by the volume) versus E for $N_f = 1, 2, 3$ and 4 respectively. I calculated the effective fermionic action for 15 bare quark masses in $m \in [0, 0.1]$, but only illustrate 3 of them. Statistical errors are less than $O(1/V) = O(10^{-5})$ and invisible at the scale of the figures. The shapes of the curves are quite similar, but the scales are quite different. The slope is small for small $E < 0.4$ and large $E > 0.7$, but it is big for intermediate $E \in (0.4, 0.7)$. We find $S_f^{\text{eff}} \propto N_f$, which means the effects of the dynamical quarks are proportional to the flavor number, and are significant for intermediate E .

With the density of states and the effective fermionic action, we can construct the full effective action in Eq. (6) as a function of E for any given N_f , m and β , using the Newton polynomial interpolation.

4.2 Thermodynamical observables with sea quarks

The thermodynamical quantities can be obtained by numerically integrating out the one-dimensional integrals in Eq. (9).

The mean plaquette energy E_p versus β is plotted in Fig. 8 for $m = m_{\text{sea}} = 0.01$ and different N_f . For $N_f = 2$ and $\beta = 5.7$, $E_p = 0.5771624 \pm 6.2251091 \times 10^{-4}$, consistent with Chen's HMD data $E_p = 0.577386(17)$ on the $16^3 \times 40$ in Ref. [22]. For $N_f = 4$ and $\beta = 5.4$, $E_p = 0.5642520 \pm 8.0579519 \times 10^{-4}$, consistent with Chen's HMC data $E_p = 0.560334(15)$ on the $16^3 \times 32$ in Ref. [22]. This also means that finite size effects on E_p are not significant. As seen in this figure, at some fixed β , E_p increases with N_f . The sea quark effects become most important around $E_p \approx 0.5$. We can understand this phenomenon by looking at Figs. 4,5,6 and 8 from which one observes maximum slope around $E \approx 0.5$. The lighter the quark mass, the bigger the slope is. Therefore, we have a mechanism: the sea quark effects reach their maximum where the effective fermionic action versus the gauge energy has a maximum slope.

Figure 9 shows the data for E_p in the chiral limit $m = m_{\text{sea}} = 0$ and different N_f . This quantity has been very useful for analyzing the chiral properties of the QED system [23]. We believe it will also be useful for QCD.

Figure 10 depicts $\langle \bar{\psi}\psi \rangle$ versus m at $\beta = 5.5$ for different N_f . The data from the Langevin algorithm [24] on the $8^3 \times 18$ lattice are also included for comparison. (The minor difference between our $N_f = 2$ data and those in [24] might be accounted by different lattice sizes used or systematic error involved). Again, one sees $\langle \bar{\psi}\psi \rangle$ decreases significantly with N_f .

4.3 Correlation between the chiral condensate and gauge action in the chiral limit

The correlation function between the plaquette and the chiral condensate indicates the interaction between sea quarks and gluons. In the quenched case, it is zero, while for full

QCD, it is not. It can be computed by measuring the mass derivative of the plaquette mean value, since

$$\frac{\partial E_p}{\partial m} = \frac{V N_c N_f}{4} \left(\frac{\langle \bar{\psi} \psi \text{ Re Tr} U_p \rangle}{N_c} - \langle \bar{\psi} \psi \rangle E_p \right) \quad (22)$$

where

$$\bar{\psi} \psi = \frac{1}{V N_c} \text{Tr} \Delta^{-1}. \quad (23)$$

A direct calculation of the r.h.s. of Eq. (22) needs very high statistics. Also it is impossible to calculate the r.h.s. when $m = 0$ because on a finite lattice $\langle \bar{\psi} \psi \rangle$ vanishes identically in this limit. However, the l.h.s. of Eq. (22) can easily be calculated in our method. Figure 11 plots the results E_p versus m for different β and N_f . The mass derivative is obtained by a linear fit to the data, which results at $m = 0$ are given in Tab. I.

5 OUTLOOK

In this paper, I have extended the microcanonical fermionic average method [15] to QCD in 3+1 dimensions, which allows us to search the parameter space (N_f, β, m) with much lower computational cost. I have provided new data for the mean value of chiral condensates $\langle \bar{\psi} \psi \rangle$, plaquette energy E_p , and their correlation function, including the results in the chiral limit for the latter two quantities.

The disadvantages of the method is that it is not easy to calculate physical observables beyond the thermodynamical quantities (e.g. the spectrum). The storage of the eigenvalues of the fermionic matrix needs big hard disk space. Although the method is applicable to the chiral limit, the systematic errors become larger when the flavor number and β are larger, and the quark mass is smaller.

As the algorithm [15] has been useful for analyzing the QED phase structure, I believe the method developed in this work will also be useful for QCD. Since the algorithm also works in the chiral limit, the study of spontaneous chiral symmetry breaking [25] will be an interesting application of this work and will be reported elsewhere.

Acknowledgments

I thank D. Chen for his HMC and HMD data, which have been used for comparison with the work done in this paper. I am grateful to E.B. Gregory for useful discussions. This work is supported by the projects of National Science Fund for Distinguished Young Scholars (19825117), National Natural Science Foundation, Guangdong Provincial Natural Science Foundation (990212), Ministry of Education, Ministry of Science and Technology, and the Foundation of Zhongshan University Advanced Research Center.

References

- [1] K. Symanzik, Nucl. Phys. **B226** (1983) 187.
- [2] H. W. Hamber and C. M. Wu, Phys. Lett. **B133** (1983) 351.
- [3] P. Hasenfratz and F. Niedermayer, Nucl. Phys. **B414** (1994) 785.
- [4] G. P. Lepage, hep-lat/9607076.
- [5] X.Q. Luo, Q. Chen, G. Xu and J. Jiang, Phys. Rev. **D50** (1994) 501.
- [6] X.Q. Luo, Comput. Phys. Commun. **94** (1996) 119.
- [7] X.Q. Luo, S. Guo, H. Kroger and D. Schütte, Phys. Rev. **D59** (1999) 034503.
- [8] J. Jiang, X.Q. Luo, Z. Mei, H. Jirari, H. Kröger and C. Wu, Phys. Rev. **D60** (1999) 014501.
- [9] S. R. Sharpe, Phys. Rev. **D46** (1992) 3146.
- [10] C. W. Bernard and M. F. Golterman, Phys. Rev. **D46** (1992) 853.
- [11] S. Aoki *et al.* [CP-PACS Collaboration], Phys. Rev. Lett. **84** (2000) 238.
- [12] S. Duane, A. D. Kennedy, B. J. Pendleton and D. Roweth, Phys. Lett. **B195** (1987) 216.
- [13] S. Gottlieb, W. Liu, D. Toussaint, R. L. Renken and R. L. Sugar, Phys. Rev. **D35** (1987) 2531.
- [14] R. Altmeyer, K. D. Born, M. Gockeler, R. Horsley, E. Laermann and G. Schierholz [MT(c) collaboration], Nucl. Phys. **B389** (1993) 445.
- [15] V. Azcoiti, G. di Carlo and A. F. Grillo, Phys. Rev. Lett. **65** (1990) 2239.
- [16] R. Petronzio and E. Vicari, Phys. Lett. **B248**, 159 (1990).
- [17] N. Cabibbo and E. Marinari, Phys. Lett. **B119** (1982) 387.
- [18] F. R. Brown and T. J. Woch, Phys. Rev. Lett. **58**, 2394 (1987).
- [19] C. Lanczos, J. Res. Natil. Bur. Stand. **B49** (1952) 33.
- [20] J. Cullum and R. Willoughby, J. Comput. Phy. **44** (1981) 329.

- [21] I. Barbour, N. Behilil, P. Gibbs, G. Schierholz, and M. Teper, in *The Recursion Method and its Applications*, edited by D. Pettifor and D. Wearie, Solid State Sciences Vol. 58 (Springer, New York, 1985), p. 149.
- [22] D. Chen, Ph. D thesis, Columbia University, (1996).
- [23] V. Azcoiti, G. di Carlo and A. F. Grillo, Mod. Phys. Lett. **A7** (1992) 3561.
- [24] M. Fukugita, S. Ohta, Y. Oyanagi and A. Ukawa, Phys. Lett. **B191** (1987) 164.
- [25] V. Azcoiti, V. Laliena and X.Q. Luo, Phys. Lett. **B354** (1995) 111.

Table 1: Mass derivative of the mean plaquette energy at $m = 0$ for $\beta = 5.2$.

N_f	$\partial E_p / \partial m$
0	0
1	-0.0357841 ± 0.0003783
2	-0.0815237 ± 0.001083
3	-0.327659 ± 0.0182
4	-0.306373 ± 0.000517

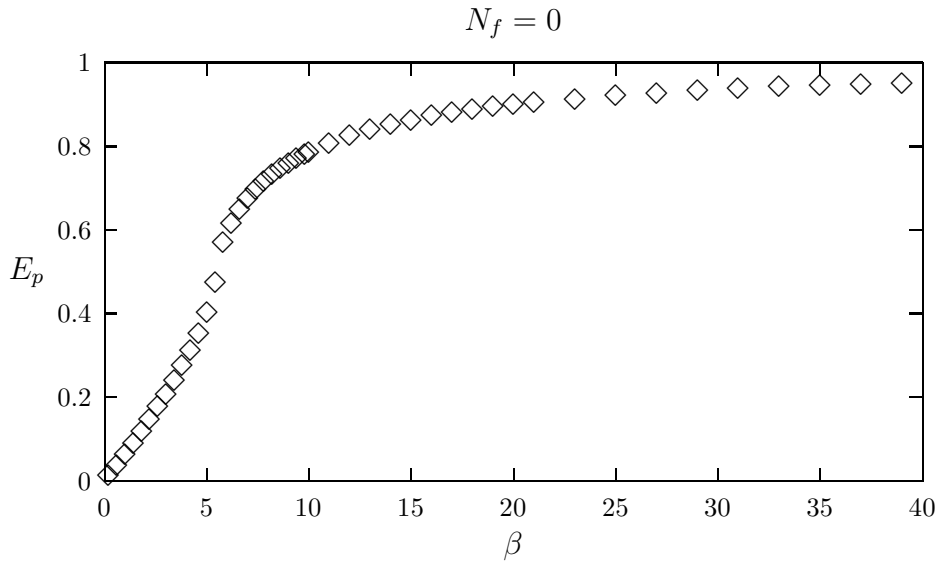


Figure 1: The vacuum expectation value of the plaquette energy from quenched simulation.

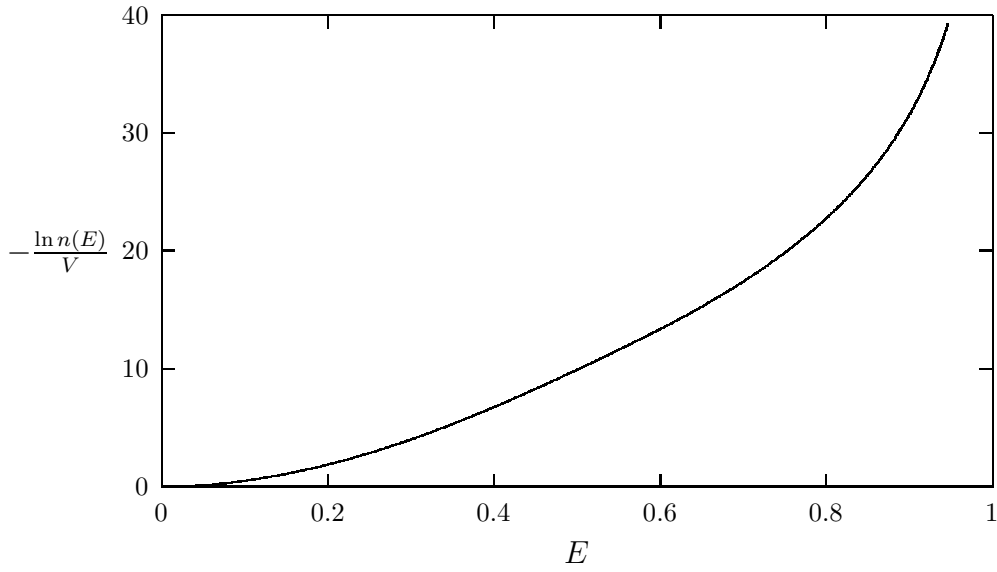


Figure 2: $-\ln[n(E)]/V$ as a function of E .

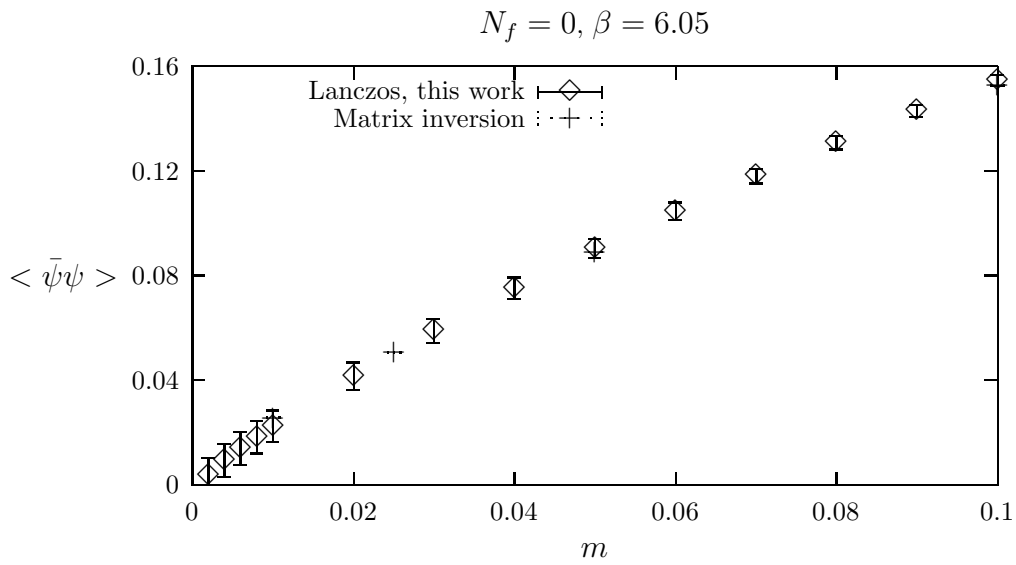


Figure 3: The quenched chiral condensate $\langle \bar{\psi}\psi \rangle$ versus m at $\beta = 6.05$.

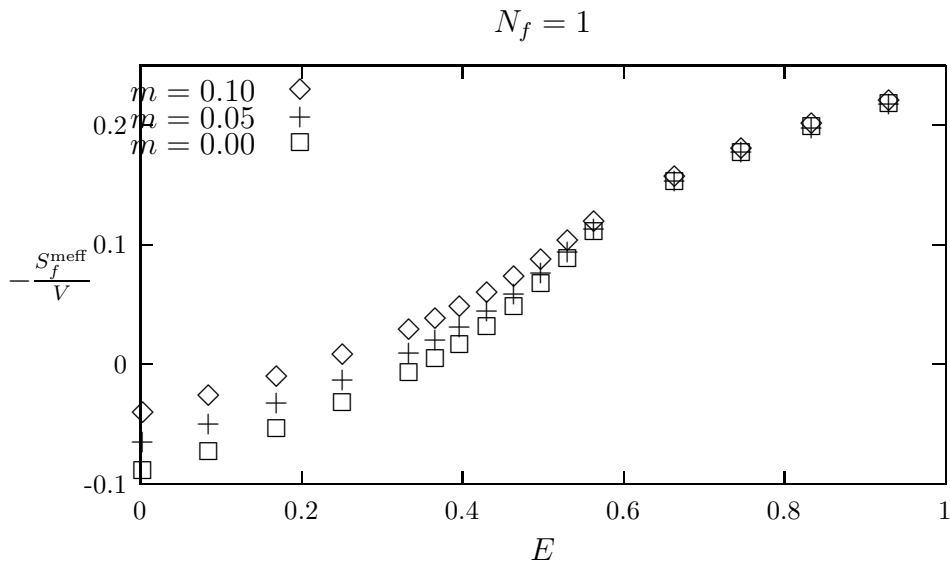


Figure 4: $-S_f^{\text{eff}}/V$ as a function of E for $N_f = 1$.

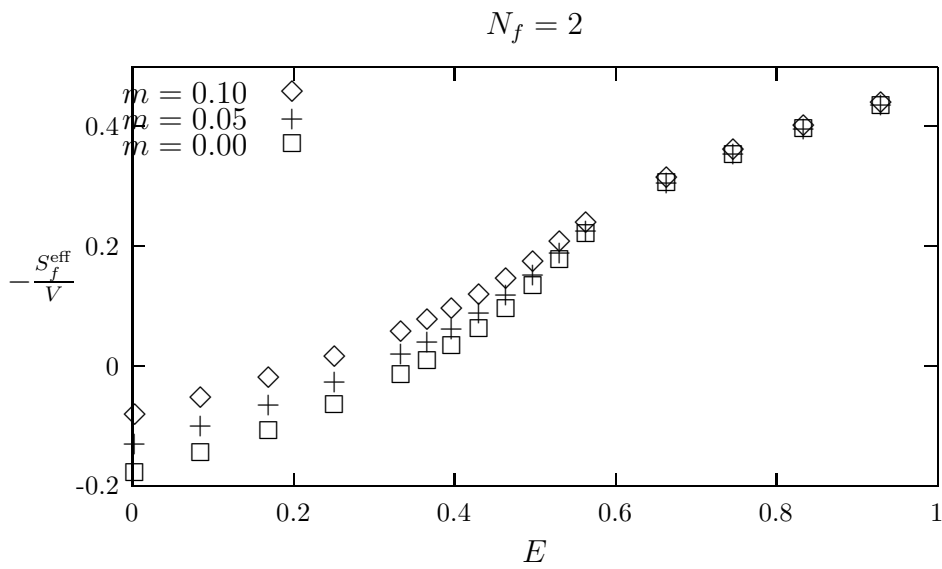


Figure 5: $-S_f^{\text{eff}}/V$ as a function of E for $N_f = 2$.

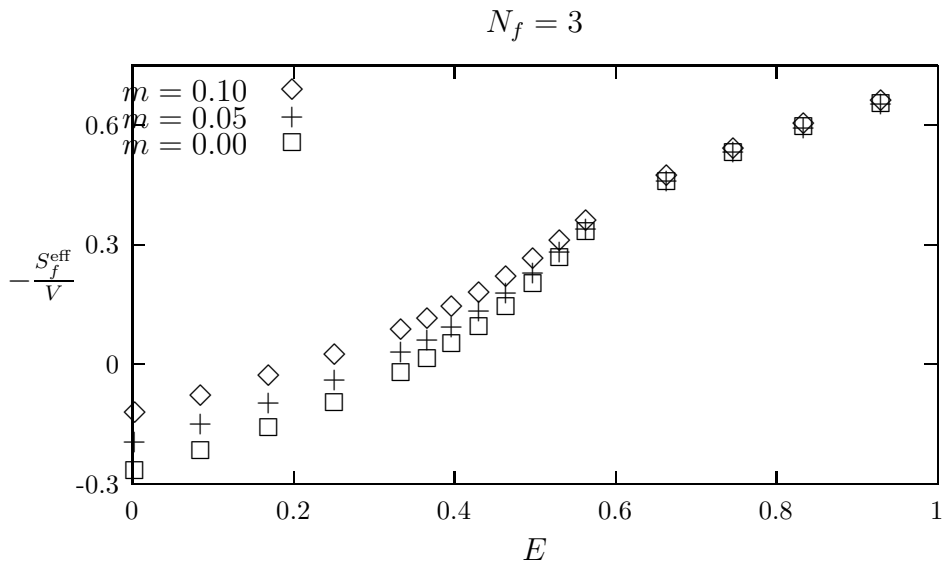


Figure 6: $-S_f^{\text{eff}}/V$ as a function of E for $N_f = 3$.

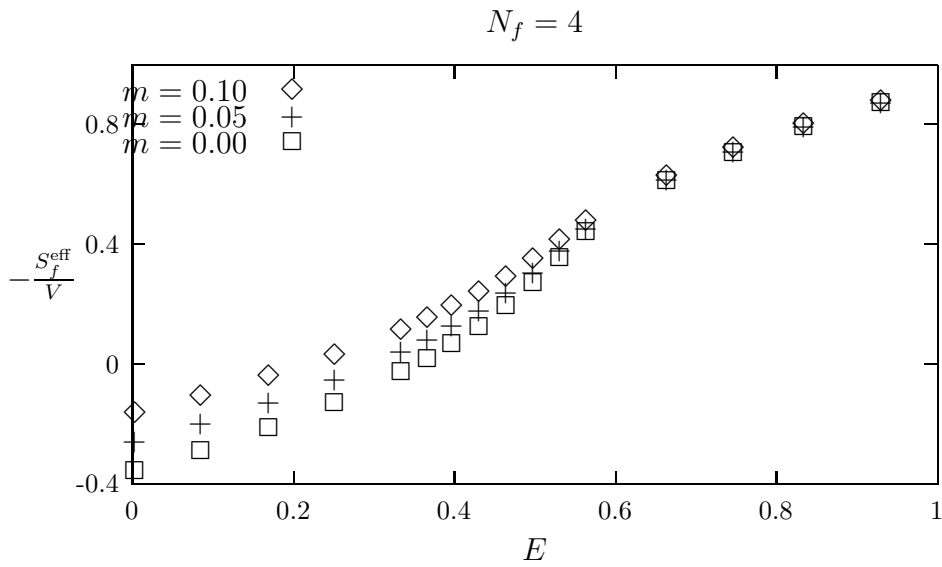


Figure 7: $-S_f^{\text{eff}}/V$ as a function of E for $N_f = 4$.

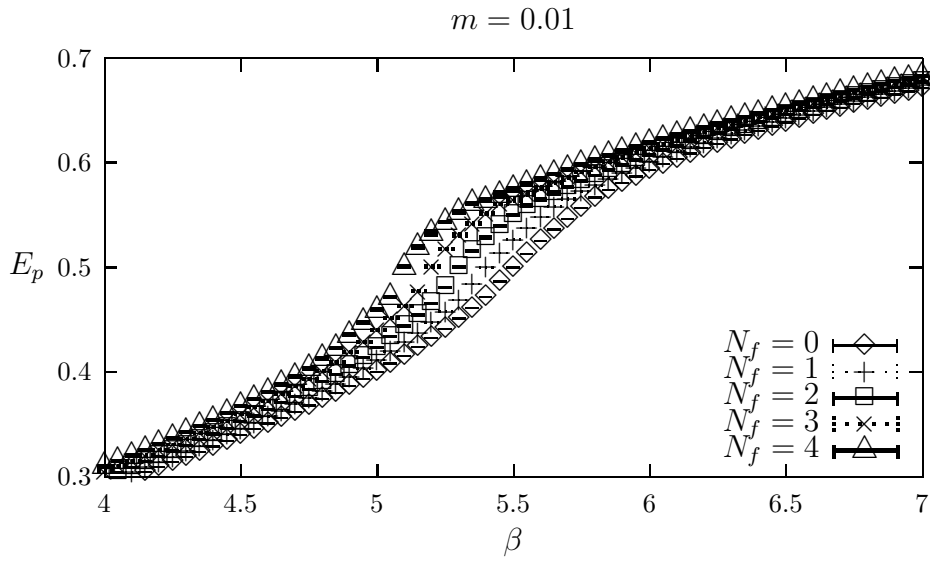


Figure 8: The mean plaquette energy E_p versus β at $m = 0.01$.

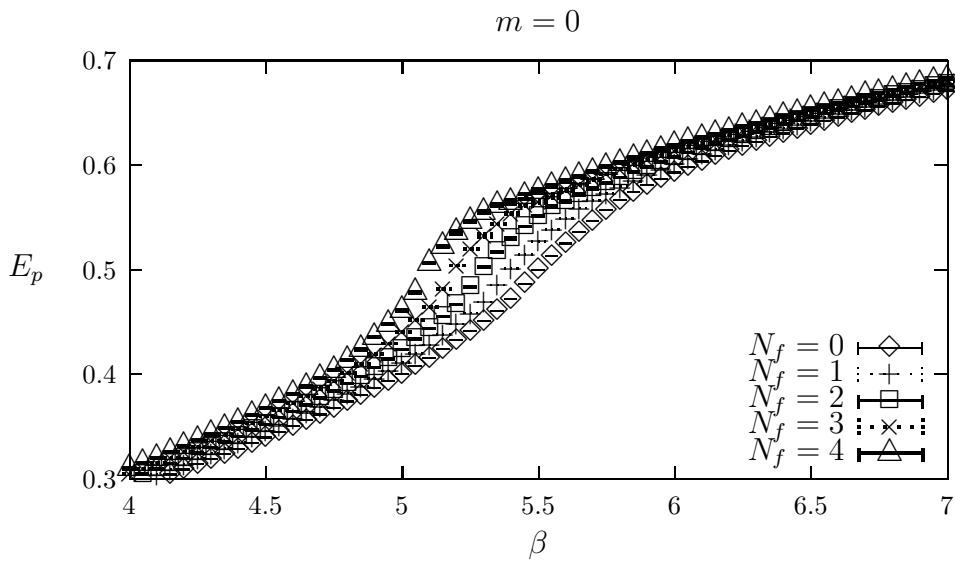


Figure 9: The mean plaquette energy E_p versus β at $m = 0$, obtained by the method described in this paper.

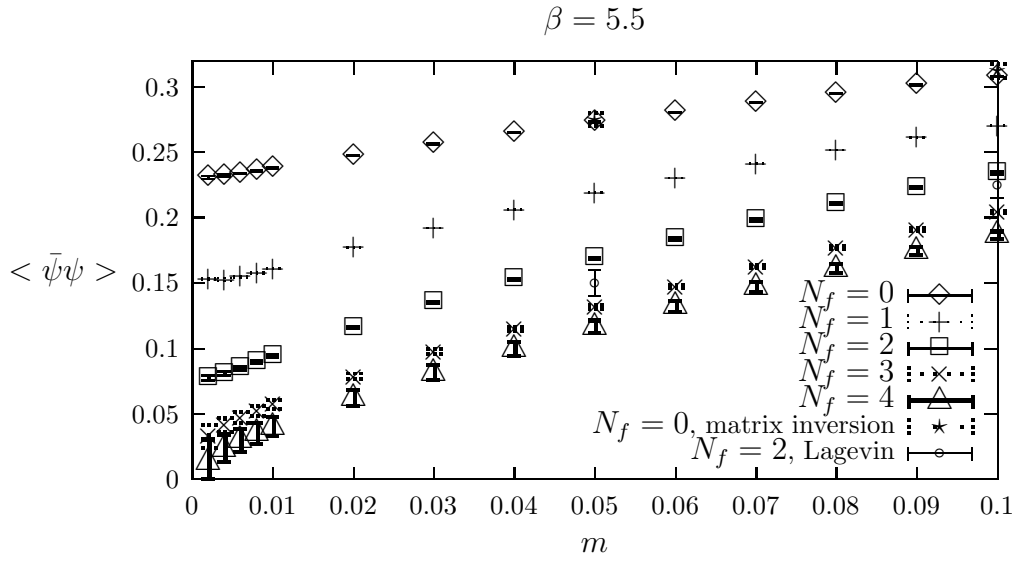


Figure 10: Chiral condensate $\langle \bar{\psi}\psi \rangle$ versus m at $\beta = 5.5$.

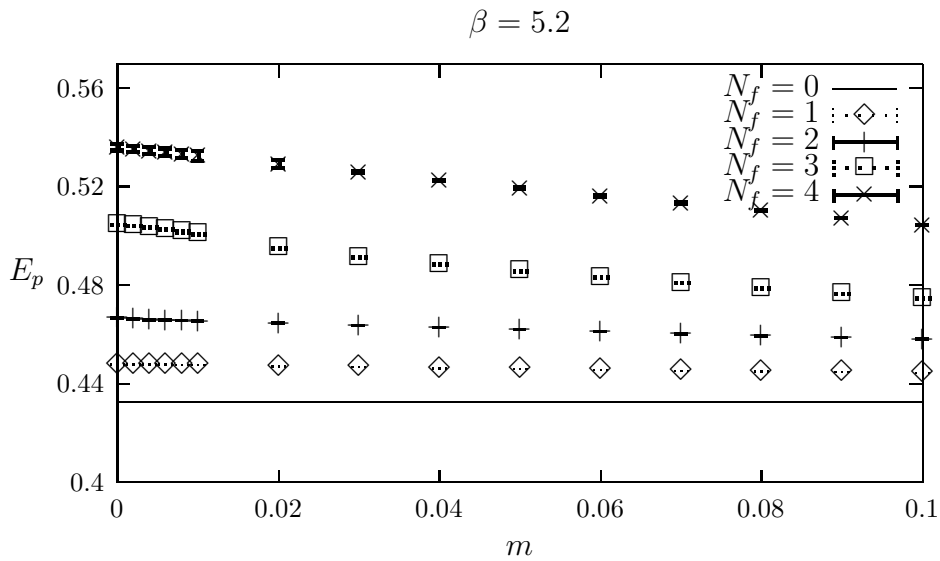


Figure 11: E_p versus m at $\beta = 5.2$.